# Anisotropic Radiation-Induced Conductivity in Oriented Poly(di-*n*-hexylsilylene) in the Solid Phase and in the Mesophase

**Garrelt P. van der Laan, Matthijs P. de Haas, and Andries Hummel**

*Radiation Chemistry Department, IRI, Delft University of Technology, Mekelweg 15, 2629 JB Delft, The Netherlands*

**Holger Frey, Sergej Sheiko,† and Martin Möller*,†**

*Center of Materials Research and Department of Chemical Technology, University of Twente, Postbus 217, 7500 AE Enschede, The Netherlands*

*Received July 8, 1993; Revised Manuscript Received December 14, 1993*•

ABSTRACT: Poly(di-*n*-hexylsilylene) (PDHS) was highly oriented by concurrent gel crystallization with UHMW-PE and subsequent ultradrawing. The orientation of the polysilylene molecules in the ultradrawn blends was demonstrated with polarized UV spectroscopy. The radiation-induced conductivity was measured, using the pulse radiolysis time-resolved microwave conductivity (TRMC) technique. Charge transport was studied both parallel and perpendicular to the polysilylene backbones. Mobilities of the charge carriers in the direction of these backbones are at least an order of magnitude higher than those perpendicular to them. The sum of the mobilities of the mobile charge carriers in the solid phase of PDHS at room temperature is at least $3 \times 10^{-5}$ $m^2$ $V^{-1}$ $s^{-1}$ in the direction of the polysilylene backbone. The magnitude of the radiation-induced conductivity in the solid phase is related to the crystallinity of the sample and decreases at the solid to mesophase transition in all systems studied. The PE matrix appears to restrict the crystallization of the PDHS backbone in the all-trans conformation in the solid phase.

## Introduction

Considerable research effort is being focused on the preparation and characterization of ordered polymeric architectures[1-5] at present. Highly organized conducting or semiconducting polymeric materials are explored because of their potential for functional applications. A basic problem in this context is the evaluation of the intrinsic electrical conductivity of the polymer chains. If charge carrier transport takes place along the polymer backbone, this should result in an anisotropic conductivity in oriented samples, similar to the anisotropic conductivity and the anisotropic optical properties found, e.g., in polyacetylene[6,7] and polyethylene (PE).[8,9]

Polysilylenes (IUPAC) or polysilanes are catenated Si polymers and are considered to be one-dimensional (1D) semi- and photoconductors.[10] On the basis of their electronic and charge transport properties, applications in microlithography,[11] electophotography,[12-15] display fabrication,[16] data storage,[17] and nonlinear optics[18-20] have been proposed. Comparable to conjugated $\pi$-systems,[22] the $\sigma$-conjugation[21] of the polymer backbone is conformation dependent and leads to intense UV absorption of the polymers in solution and in the solid state. A band gap of about 4 eV[12] is typical for polysilylenes.

The crystal structure of symmetrically substituted poly(di-*n*-alkylsilylene)s depends on the side-chain length.[10] In the highly ordered low-temperature solid phase (phase I) of poly(di-*n*-hexylsilylene) (PDHS), the silicon backbone adopts an all-trans conformation[23] with the side chains oriented perpendicular to the main chain. Upon heating, the side chains "melt" and the polymer backbone becomes conformationally disordered, forming a mesophase (phase II) consisting of hexagonally packed, conformationally disordered macromolecules.[23,24] A similar phase behavior is also found for a number of other polymers with flexible molecular backbones, such as polysiloxanes[25] and polyphosphazenes.[26]

Gel technology provides a special and easy route to prepare blends of incompatible crystalline polymers[27] with an ultrafine dispersion. Typically, crystalline polymers do not cocrystallize or form eutectic mixtures. However, in dilute or semidilute solutions, as used in the gel preparation, the gel crystallization of one polymer will be little affected by the presence of a second component. Particular advantages can be gained when polysilylenes are blended with ultrahigh molecular weight polyethylene (UHMW-PE) by gel crystallization.[28] Solid-state drawing of dried gels of UHMW-PE results in the transformation of the chain-folded lamellae to a chain-extended fibrillar structure, yielding highly oriented ultrastrong fibers or films.[29] At the temperatures employed for drawing UHMW-PE to high extensions, most poly(di-*n*-alkylsilylenes) are in the mesomorphic state (phase II), which can also be classified as a columnar liquid crystalline phase.[21]

In the liquid crystalline phase, polysilylenes can be deformed by applying a relatively small stress. Consequently, polysilylene domains within a matrix of another polymer do not impose restrictions on mechanical processing as long as the processing temperature is above the I → II disordering transition. Thus, highly oriented PE/PDHS blends can be prepared by the following steps: (i) the PDHS has to be dispersed homogeneously in nanometer-sized domains in the PE matrix; (ii) the blends have to be oriented above the I → II disordering temperature of PDHS. This method of cocrystallization and subsequent reorientation of photoconductive or electroactive polymers in insulating polymer host materials enables one to combine the advantageous properties of the electroactive polymer with good stability and processability of the polymeric host. We have shown previously that poly(di-*n*-pentylsilylene) (PDPS) can be dispersed in nanometer domains in gels of UHMW-PE[28] by concurrent gel crystallization. By stretching the dried gels to draw ratios of 30 or more at elevated temperature above the I → II transition of PDPS, PE films containing highly aligned

† Present address: Organische Chemie III/Makromolekulare Chemie, Universität Ulm, D-89069 Ulm, Germany.

• Abstract published in *Advance ACS Abstracts*, February 15, 1994.

0024-9297/94/2227-1897$04.50/0 

PDPS were obtained. The present work is directed toward the preparation and characterization of such highly oriented films to investigate the anisotropic conductivity of poly(silylene)s.

Poly(di-*n*-hexylsilane) (PDHS) was selected as the polysilylene component for several reasons. PDHS displays a solid to liquid crystalline transition (I → II) at 42 °C, thus allowing the orientation method mentioned above to be applied at only slightly elevated temperatures. The radiation-induced conductivity of long-lived (microseconds) mobile charge carriers in unoriented PDHS has been studied in previous investigation.[30,31] Little difficulty was expected in separating the DPHS conductivity signal from the short-lived (nanoseconds) conductivity signal that was reported earlier in UHMW-PE.[8,9] The I → II transition of PDHS is accompanied by a loss in backbone $\sigma$-conjugation as is indicated by a thermochromic blue shift of the UV absorption band from 372 to 315 nm[32] as well as by a decrease of the charge carrier mobility by more than 1 order of magnitude.[30,31] This makes it possible to study the effect of blending and subsequent drawing on the I → II transition of PDHS by measuring the UV spectra at different temperatures and studying the temperature dependence of the radiation-induced conductivity.

We will demonstrate that charge transport in PDHS takes place preferentially along the catenated Si backbones. Furthermore, we investigated the temperature dependence of the radiation-induced conductivity in PDHS in a UHMW-PE matrix before and after orientation by drawing of the blend. The results are compared with those obtained with pure PDHS.

Pulse radiolysis with 3 MeV of electrons results in charge carrier formation throughout the sample. With the TRMC method,[33] charge carrier transport is studied by monitoring the radiation-induced microwave conductivity of the sample. The displacement of the charge carriers due to the oscillating electric field during one period is considerably less than the smallest (nanometer) dimensions of the PDHS regions. Due to the contactless nature of the TRMC method, inhomogeneous materials can be studied without the electrode contact problems or boundary effects encountered commonly with drift mobility experiments. Thus, the radiation-induced conductivity of PDHS embedded in a PE matrix can be measured. Transients can be determined from samples with the monitoring field of the microwaves parallel or perpendicular to the oriented polysilylene backbones present in the drawn PE/PDHS films. From the radiation-induced conductivity, a lower limit for the charge carrier mobility can be given.[30]

Highly oriented polysilylenes may be considered as a 1D model system to gain insight into the mechanism of charge migration in polymeric semiconductors. For polysilylenes with *n*-pentyl to *n*-octyl side chains, we have demonstrated that the mobility of radiation-induced charge carriers is strongly dependent on the polysilylene backbone conformation.[31] This together with the effect of the side-chain length on the decay kinetics of the radiation-induced conductivity led us to the hypothesis that charge carriers in crystalline polysilanes move preferentially along the catenated Si backbones.[31]

For the all-trans conformation of PDHS in the solid phase[30] (with an isotropic distribution of backbone orientations) we reported a lower limit for the charge carrier mobilities of $1.5 \times 10^{-5}$ m$^2$ V$^{-1}$ s$^{-1}$, which is considerably larger than the value reported from time-of-flight studies.[34]

## Experimental Section

**Polymers.** UHMW-PE (HIZEX 240 M, $M_w = 1.5 \times 10^6$) was employed as a reactor powder. Di-*n*-hexyldichlorosilane was prepared via a Grignard reaction, and the purity was found to be better than 99% according to gas chromatography. High molecular weight PDHS was prepared by reductive coupling of the monomers in a dispersion of sodium in toluene/isooctane as described elsewhere.[35] The PDHS was precipitated from toluene by adding methanol. The weight-average molecular weight of PDHS as determined by GPC referenced to narrow polystyrene standards was found to be $5.1 \times 10^5$. $M_w/M_n$ ranged between 2 and 3, which is typical for the Wurtz-type coupling reaction.[36]

**UHMW-PE/PDHS Gel.** The gel was prepared by dissolving 3 parts of UHMW-PE and PDHS in an 80:20 ratio in 97 parts of *m*-xylene at 130 °C. Lowering the temperature to 120 °C resulted in the formation of an opaque gel, which was dried, compressed, and finally annealed under vacuum at 60 °C to remove xylene completely. The dry blend was pressed to remove voids.[37] With this procedure, opaque samples of about 1-mm thickness were obtained. The blend was cut into strips, which were drawn to films with draw ratios $\lambda$ between 10 and 70, below the actual limiting draw ratio of ca. 100. TRMC experiments were performed on samples with $\lambda$ = 30–40.

**TEM and SFM.** Micrographs of the blend were recorded by means of a Zeiss EM 902 electron microscope. For this purpose a small specimen of the PE/PDHS blend was embedded in an EPON resin and stained with $RuO_4$. Ultrathin sections were obtained with an Ultracut E ultramicrotome (Reichert and Jung), which was equipped with a diamond knife.

The scanning force (SFM) micrographs were recorded using a Nanoscope II (Digital Instruments, Santa Barbara, CA). Commercial $Si_3N_4$ pyramidal tips were mounted on a cantilever with force constant of 0.06 N/m.

**UV Spectroscopy.** UV dichroism experiments on the oriented films were carried out on a Perkin-Elmer Lambda 9 spectrophotometer equipped with polarizers transparent in the region from 215 nm to 2.3 $\mu$m. Other UV measurements were recorded by means of a UVIKON 930 spectrometer.

**Time-Resolved Microwave Conductivity (TRMC) Measurements.** The microwave system used consists of a waveguide of internal cross section $3.55 \times 7.1$ mm, and the frequencies used were in the Ka band (26.5–38 GHz). The sample were placed in a piece of waveguide (the cell) closed at one end with a copper plate. The top wall of the cell was reduced to 0.4-mm thickness to minimize attenuation of the electron beam. A length of ca. 10 mm of the samples was irradiated with 3 MeV of electrons from a Van de Graaff accelerator using pulses of 5–50-ns duration and beam currents of 4 A. The penetration depth of the primary 3 MeV of electrons is 15 mm in 1 g/cm$^3$ material. Irradiation of the 3.5-mm-thick samples resulted in an energy deposition uniform within 10%. The energy absorbed in the sample per unit volume (dose) was determined to be 120 kJ/m$^3$ for a 50-ns pulse, using Far West Technology-92 radiochromic thin film dosimeters.[38]

The radiation-induced conductivity was monitored by time-resolved measurement of the change in reflected microwave power by the sample.[33,39,40] The time scale of detection of the experiments was from nanoseconds to milliseconds. For small variations in the conductivity, the change in reflected microwave power is directly proportional to the change in conductivity of the sample. The frequency dependence of the TRMC transients can be fitted to determine the absolute magnitude of the conductivity.[33]

The presence of air in the cell leads to large short-lived (nanoseconds) radiation-induced conductivity signals due to free electrons formed in the gas phase. The cell was flushed with $SF_6$, which considerably depressed this signal by acting as an ultrafast scavenger for free electrons.

**Effect of Accumulated Dose.** Upon irradiation with UV light, $\gamma$-quanta, and high-energy electrons, polysilylenes are degraded, e.g., via homolytic scission or silylene elimination.[41-43] For PDHS the *G* values for chain scission and cross-linking are reported to be 0.42 and 0.04 per 100 eV absorbed, respectively.[44] The maximum total accumulated dose used for the experiments presented in this paper was ca. 20 kGy. Therefore, a maximum concentration of ca. 1 mM of radiation-induced damage to the polymer backbones should occur. We have found that both the end-of-pulse conductivity and the first half-life of the conductivity decay are in fact almost unchanged (<10%) after a total

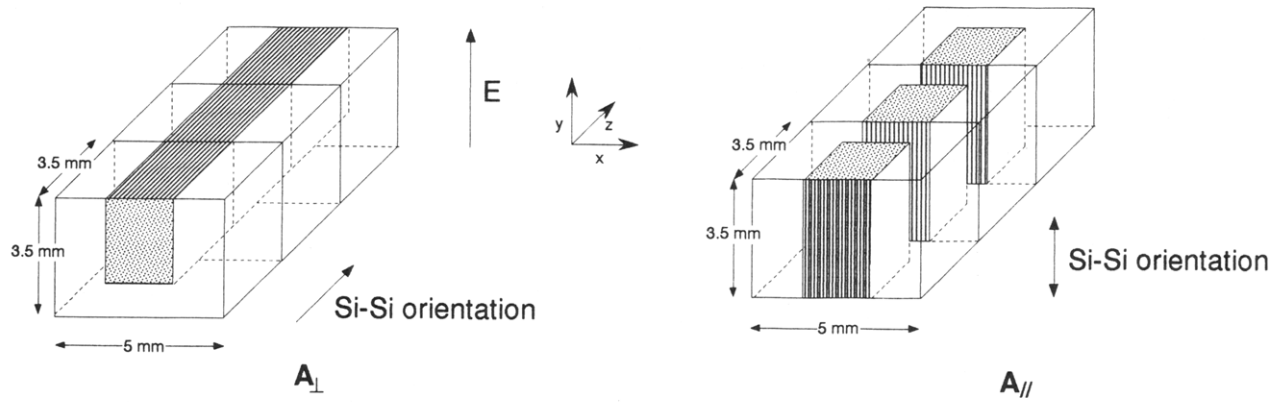


**Figure 1.** Schematic drawing of the samples used for the anisotropy experiments. Both samples consist of three identical blocks. The oriented PE/PDHS films are in the shaded part surrounded on three sides by polyester resin. Shown is the arrangement of sample $A_\perp$ with the polysilylene backbones (i.e., Si–Si orientation) perpendicular to the microwave field (↑E) and the arrangement of sample $A_\parallel$ with the polysilylene backbones parallel to ↑E.

accumulated dose of 20 kGy. At considerably higher accumulated doses (up to 200 kGy) marked decreases of both the magnitude and half-life of the conductivity transients are, however, observed.

**Sample Preparation for TRMC Experiments.** Drawn PE/PDHS films ($\lambda$ = 30–40, dimensions ca. 4 × 300 mm) were used in samples A and B. The sample with the PDHS backbones aligned (sample A) was prepared by winding drawn PE/PDHS films one by one around a thin brass yoke. The distance between legs of the yoke was ca. 50 mm. The thickness of the compressed film bundle was approximately 0.8 mm. The orientation of the PE/PDHS films was fixed in a polyester resin (Alpolit SUP832; Hoechst). The resin was selected because of its small volume change on hardening. However, it showed a high dielectric loss at microwave frequencies. Therefore, after polymerization, the amount of resin material was reduced as much as possible without destroying the mechanical integrity. To be able to turn the sample in the microwave cell and hence change the orientation of the polymer backbones with respect to the microwave field, blocks of 5 × 3.5 × 3.5 $mm^3$ were cut with the fiber orientation along one of the short axes.

Three of the blocks containing the aligned films of PE/PDHS, of total weight ca. 15 mg (3 mg of PDHS), were placed in the cell. Two LDPE films of 1-mm thickness were placed on either side of the blocks to center the sample and to minimize the amount of air in the cell. LDPE is known to give no conductivity transient in pulse radiolysis TRMC experiments. The blocks were placed in the microwave cell with the orientation of the polymer chains either perpendicular (Figure 1, sample $A_\perp$) or parallel (Figure 1, sample $A_\parallel$) with respect to the applied electric field of the microwaves. The accuracy of orientation with respect to the field of the microwaves in the cell was estimated to be between 3 and 5 degrees.

Sample B consists of a wad of drawn PE/PDHS film without preferential orientation of the film. Sample C of undrawn PE/PDHS blend. For samples B and C only 20 mg was available. Therefore, a PMMA block with dimensions to fit the microwave cell with a small cavity for the sample was used to optimize the position of these small samples in the cell. PMMA is known to give no radiation-induced conductivity signals.

Sample D consists of ca. 200 mg of pure PDHS compressed to ca. 11 mm in the cell.

## Results and Discussion

**Blending and Orienting of PE/PDHS Samples.** To verify the content of PDHS and the homogeneity of the blend, elementary analysis of the area of the dried blend also used for the experiments was performed. The Si content of the 80/20 PE/PDHS blend was found to be 2.72 mass %, close to the value of 2.84 mass % expected for a 80/20 PE/PDHS blend. The blend consisted of small PDHS crystallites in a matrix of polyethylene as shown in Figure 2 for a blend prepared from a 80:20 UHMW-PE/PDHS gel. The electron micrograph shows that PDHS crystals of width between 20 and 130 nm are embedded between layers of the lamellar crystals of polyethylene. The PE lamellae in the blends appear to be unaffected by the polysilylene component.

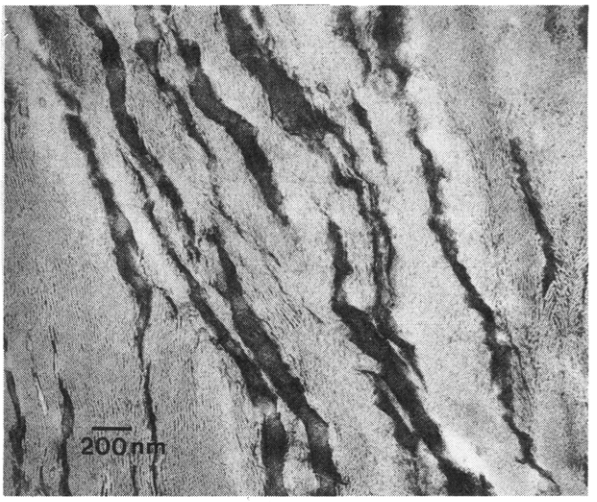


**Figure 2.** TEM micrograph of undrawn PE/PDHS blend. The dark areas are poly(di-*n*-hexylsilylene) domains of 20–60-nm width imbedded in polyethylene lamellae. The blends were stained with $RuO_4$.

The PE/PDHS blend could be drawn to draw ratios up to 100; the drawing procedure was similar to drawing of pure UHMW-PE. The resulting films were transparent and appeared slightly more flexible than pure PE films. They showed the strong fluorescence typical of PDHS. The fibrillar structure of the untreated surface of the drawn films was studied by scanning force microscopy (SFM) and compared with stretched samples of pure UHMW-PE. In Figure 3 a typical SFM image of a PE/PDHS film is shown, recorded from a highly stretched film with draw ratio $\lambda$ = 70. The image is identical with the SFM results obtained for ultradrawn fibers of pure PE[45] and shows the fibrillar elements of the film; PE and PDHS are indistinguishable. No nonoriented regions or perturbations can be observed. On the basis of the average width of 60 nm of the PDHS domains in the undrawn blend (Figure 2), the minimum width of the PDHS regions perpendicular to the drawing direction in drawn films with $\lambda$ = 30 is estimated to be ca. 10 nm. The interchain distance in the hexagonally packed mesophase of PDHS is 1.2 nm. While PDHS domains may be considered to exist, large interfacial areas will also be present between PE and PDHS.

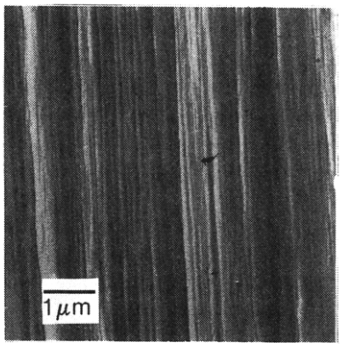


**Figure 3.** SFM image of the fibrillar structure of the surface of an 80/20 PE/PDHS film with λ = 70. The depicted fibers have lateral dimensions of approximately 100 nm.

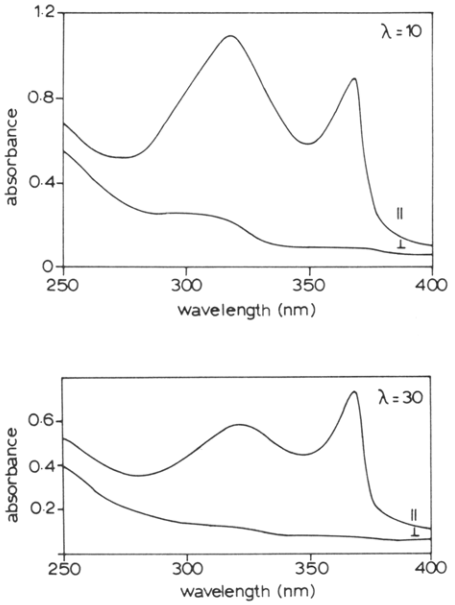


**Figure 4.** Orientation of PDHS in drawn PE/PDHS films shown by the polarized UV absorption spectra of oriented 80/20 PE/PDHS films. A film with λ = 10 is shown above, and a film with λ = 30 is shown below.

The drawn films were studied by polarized UV spectroscopy to characterize the extent of molecular order and orientation. Strongly dichroic behavior of PDHS has been reported previously for films deposited and stretched on a polymeric substrate.[46] Polarized UV spectra recorded parallel and perpendicular to the drawing direction of films with λ = 10 and 30 are shown in Figure 4. Both absorption bands at 320 nm (disordered backbone) and 370 nm (all-trans backbone) are present, although the spectra were recorded below the disordering transition.

The UV absorption is strongly dichroic, similar to drawn blends of PE/poly(di-*n*-pentylsilylene).[28] For λ = 10, the orientation of the PDHS is already very distinct. However, the orientation of the PDHS is not complete, as is demonstrated by the band at 320 nm that is present in the spectra recorded for both orientations. A draw ratio of λ = 30 leads to extremely strong dichroism for the whole absorption region. Therefore, we assume that the polysilylene chains are fully aligned when λ = 30. Higher draw ratios lead to fibers that are more difficult to process but do not lead to an increased dichroism. Therefore, for the change transport measurements, oriented PDHS films with a draw ratio λ = 30–40 were used.

Heating of the drawn PE/PDHS blends above the disordering transition did not result in complete disappearance of the 370-nm absorption band as was found for the undrawn material even at 80 °C far in the mesophase regime. Evidently, melting of the side chains and conformational changes in the backbone are influenced by the presence of the PE–PDHS interface and the micromechanical constraints affecting the PDHS chains.

**Table 1. Phase I→II Transition Enthalpies, $\Delta H$, As Found from DSC Measurements on First and Second Heating Runs[a]**

| sample | drawing ratio | $\Delta H_{trans}$ [J/(g PDHS)] first run | $\Delta H_{trans}$ [J/(g PDHS)] second run |
|---|---|---|---|
| 100% PDHS | 1 | 65 | 65 |
| blend | 1 | 22 | 29 |
| film | 10 | 24 | 25 |
| film | 30 | 27 | 34.5 |
| film | 70 | 22.5 | 24.5 |

[a] Results are compared with $\Delta H$ of 100% PDHS (sample A).

As the radiation-induced conductivity depends strongly on the PDHS backbone conformation,[30,31] it is essential to know (i) the extent of PDHS actually present in the all-trans conformation below the I → II transition temperature and (ii) to what extent PDHS is able to transform into the disordered conformation when the blend is heated above the transition.

The crystallinity of the PDHS in the blends relative to the crystallinity of a 100% PDHS sample is calculated by comparing the disordering transition enthalpies at the I → II transition. PE/PDHS samples with various drawing ratios λ was studied by differential scanning calorimetry (Table 1). From the $\Delta H$ values, it is estimated that at most only a fraction of 34% of PDHS is crystalline in the unoriented blends and a fraction of ca. 40% in the drawn films with λ = 30. Increasing the drawing ratio to λ = 70 led to an even slightly lower $\Delta H$ value. It should be kept in mind that these are not absolute values but relative to the crystallinity of a 100 PDHS sample (sample D).

Generally the DSC results are in agreement with the temperature dependence of the polarized UV spectra, showing that in the drawn blends only a fraction of the PDHS undergoes the I → II conformational transition upon heating. The temperature dependence of the UV spectra raises the question whether the structure of PDHS in the drawn blends can still be described by a two-state model, i.e., crystalline and mesomorphic, or whether the PDHS domains become constrained to such an extent that part of the chains are forced into a new "blended" situation.

In the second heating run, the drawn films showed higher $\Delta H$ values than in the first experiment. This indicates that some rearrangement of PDHS is possible at elevated temperature, resulting in an increased crystallinity upon cooling. Some loss of orientation might also be expected after one temperature cycle. However, no annealing effect on the orientation, i.e., molecular relaxation, could be detected with polarized UV absorption measurements; thus, the effect must be small.

**Pulse Radiolysis Microwave Conductivity.** The conductivity at the end of the radiation pulse ($\Delta\sigma_{eop}$ (S/m)) is related to the sum of the mobilities of the (positive and negative) charge carriers ($\sum\mu$ ($m^2$/Vs)) and the number of electron-hole ($e^-$–$h^+$) pairs present per unit volume ($N_p$($m^{-3}$))

$$\Delta\sigma_{eop} = e\sum\mu N_p \qquad (1)$$

where $e$ is the elementary charge in coulomb. $N_p$ is related to the energy deposited per unit volume, $D$ ($Jm^{-3}$), by

$$N_p = D/I_p \qquad (2)$$

where $I_p$ is the energy required to form one ($e^-$–$h^+$) pair in joule. Using the TRMC method, mobile charge carriers present on a nanosecond time scale are detected. It is possible that a considerable fraction of the initially formed charge carriers recombines on a subnanosecond time scale. Therefore, the experimentally observed charge carrier concentration at the end of the pulse is probably smaller than $N_p$ as found from eq 2. At present is it unknown what fraction of the initially formed ($e^-$–$h^+$) pairs are observed. However, a lower limit for the sum of the mobilities ($\sum\mu_{min}$) may be obtained from eqs 1 and 2.

$$\sum\mu \geq (I_p/e)(\Delta\sigma_{eop}/D) = \sum\mu_{min} \quad (3)$$

If the pair formation energy, $I_p$, is expressed in electronvolts (and called $E_p$), then eq 3 reduces to the convenient expression

$$\sum\mu_{min} = E_p(\Delta\sigma_{eop}/D) \quad (4)$$

For PDHS it is evidenced that $E_p$ = 21 eV.[31]

From studies on linear alkanes it is known that only a fraction of ca. 3% of the initially formed ($e^-$–$h^+$) pairs escapes geminate recombination.[47] Recent computer simulations[48] have indicated, however, that the escaped fraction could be an order of magnitude larger in media with direction-dependent charge carrier mobilities. It is not sure that only charge carriers that have escaped from their original coulomb field are observed. Charge carrier pairs that are still in their mutual coulomb field but are trapped on different polysilylene backbones could also contribute to the conductivity signal. We have found that in a dilute solution of PDHS in *n*-hexane, the polymer acts as a trap for both electrons and holes that are produced in the hydrocarbon environment.[48] These effects will raise the number of charge carriers that contribute to the TRMC signal considerably, probably to a value above 10% of $N_p$ as defined in eq 2. For the present calculation of the charge carrier mobilities we take all initially formed charge carriers to contribute to the observed conductivity and therefore use eq 4 to obtain a lower limit value of $\sum\mu$.

In PE only short lived (~10 ns) charge carriers are observed using the TRMC technique. Therefore, on a longer time scale only charge carriers in the PDHS regions will contribute to the conductivity transients. The number of charge carriers that are then observed will be proportional to the energy that is absorbed in these regions. This fraction is proportional to the PDHS content of the samples. Therefore, all conductivity transients are normalized with respect to the DPHS content of the samples. This normalization is only valid if no net charge transport takes place between the PE and the PDHS regions. Below we will demonstrate this to be a valid assumption.

The method of normalization does not affect the anisotropy ratio that is experimentally determined because the conductivities of $A_\parallel$ and $A_\perp$ are measured on the same sample that was turned 90° to obtain the two orientations.

**Effect of Blending on the Radiation-Induced Conductivity.** Trace D in Figure 5 shows the radiation-induced conductivity transient obtained for pure unoriented PDHS (sample D) at room temperature. The transient demonstrates the presence of long-lived charge carriers and disperse decay kinetics of the conductivity. Trace C in Figure 5 was obtained for the undrawn 80/20 PE/PDHS blend (sample C) at room temperature. Both C and D show long-lived conductivity signals with similar disperse decay kinetics, which is taken to indicate that the conductivity in C originates from the PDHS regions in the sample. The considerably smaller conductivity that is observed in the blend could be due to the lower crystallinity of the same, as will be discussed below.

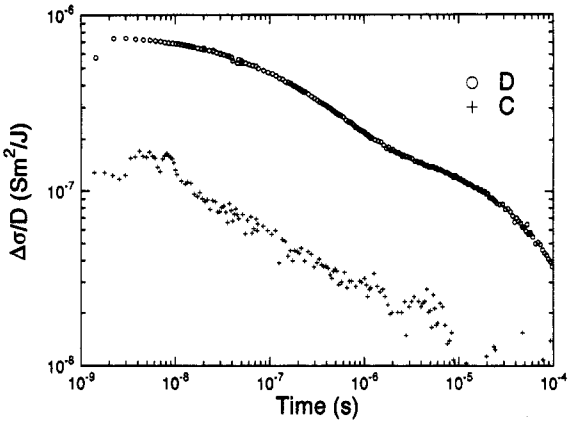


**Figure 5.** Comparison of dose-normalized radiation-induced conductivity transients taken at room temperature at 100% unoriented PDHS (sample D) and undrawn 80/20 PE/PDHS blend (sample C). Transient C has been multiplied by a factor of 5 to correct for the 20% PDHS content of the blend. Use was made of 5- and 20-ns pulses depositing ca. 12 and 48 kJ/m³, respectively. Time zero is taken as half the pulse length.

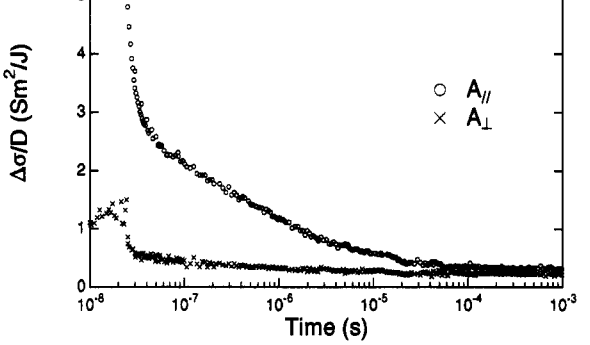


**Figure 6.** Dose-normalized radiation-induced conductivity transients obtained at room temperature on drawn (λ = 30) PE/PDHS films with the film (and thus polysilylene backbone) orientation parallel ($A_\parallel$) or perpendicular ($A_\perp$) to the microwave field. Use was made of 50-ns pulses depositing ca. 120 kJ/m³ per pulse. The signals are normalized to 100% PDHS content. Time zero is taken as half the pulse length.

Traces $A_\parallel$ and $A_\perp$ in Figures 6 represent the radiation-induced conductivity transients obtained for the drawn PE/PDHS films with the polysilylene backbones oriented parallel (sample $A_\parallel$) and perpendicular (sample $A_\perp$) to the microwave field at room temperature. After drawing, the conductivity signals demonstrate the presence of long-lived charge carriers with dispersive decay kinetics similar to that found for sample D. Therefore, we conclude that also in these samples the long-lived part of the conductivity transients originates from the migration of radiation-induced charge carriers in the PDHS regions of the samples. It should be stated that the short-lived signal during the pulse and up to 20 ns after the pulse in Figures 6 and 7 does not arise from PDHS domains in sample A as will be discussed below.

In general, blending and subsequent drawing do not seem to have a large influence on the decay kinetics of the conductivity transients. Therefore, we assume that the conductivity mechanism in the blend and the drawn films is comparable to that of bulk PDHS.

**Anisotropy.** Figure 6 clearly demonstrates the effect of orienting the sample with the aligned polysilylene

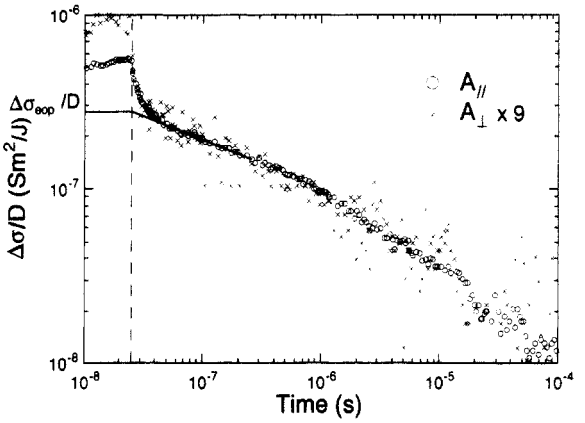


**Figure 7.** Dose-normalized radiation-induced conductivity transients of $A_\parallel$ and $A_\perp$ as shown in Figure 6 after correcting for baseline shift as discussed in the text. The $A_\perp$ transient has been multiplied by 9 to demonstrate the anisotropy ratio and similarity of the decay kinetics. Time zero is taken as half the pulse length. The solid line shows the extrapolation of the long-lived part of the transients to an end of pulse conductivity ($\Delta\sigma_{eop}/D$).

backbone either parallel ($A_\parallel$) or perpendicular ($A_\perp$) to the applied microwave field (Figure 1).

In the transients shown in Figure 6, several contributions to the radiation-induced conductivity from different components of the sample can be distinguished, each with its own lifetime: (i) a short-lived component during the pulse and up to approximately 20 ns after the pulse; (ii) a slowly decaying signal visual in the time window from approximately 20 ns after the pulse to 500 $\mu$s, with disperse, i.e., nonmonoexponential decay kinetics; (iii) an upward shift of the baseline visible after 100 $\mu$s showing no decay. These contributions are interpreted as follows.

(i) The short-lived component could originate from two effects. First, highly oriented polyethylene has been found to exhibit strongly anisotropic radiation-induced conductivity itself.[18] However, these charge carriers, which are highly mobile, have very short lifetimes of ca. 10 ns. Second, the short-lived component could also arise from small air bubbles encapsulated in the polyester resin used to fix the orientation of the film. This effect is expected to be independent of the orientation. We probably observe a combination of the two effects.

(ii) The more slowly decaying part of the conductivity signal visible within the time window from 20 ns after the pulse to 500 $\mu$s is attributed to charge carriers in the PDHS regions of the samples as discussed above.

(iii) The constant level visible after 100 $\mu$s arises from a small temperature rise of the polyester component of the sample. The polyester shows a large temperature-activated dielectric loss in the microwave frequency range due to the dipoles present. The small amount of PDHS present in these samples required a relatively high radiation dose per pulse (ca. 120 kJ/m$^3$). This relatively high dose results in a temperature increase of the sample on the order of 0.1 K, which in turn results in a slightly higher background loss of the sample after the pulse. The time necessary to dissipate the additional heat to the surroundings is much longer than the time window of the experiment. Therefore, the small temperature increase effectively results in an upward shifted baseline after the pulse. This effect is independent of orientation and has been positively verified with a 100% polyester sample.

After correcting for the baseline shift described above, we obtain an anisotropy ratio of 9 ± 1 of the radiation-induced conductivity in the PDHS regions as is demonstrated in Figure 7. Charge carrier transport is clearly

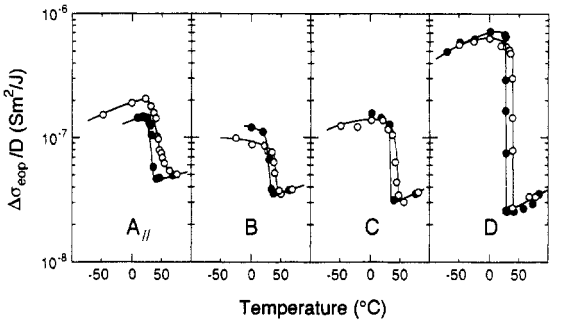


**Figure 8.** Temperature dependence of $\Delta\sigma_{eop}/D$ for $A_\parallel$, B, C, and D. All values are normalized to 100% PDHS content. Open circles are values obtained upon heating. Solid circles are values obtained upon cooling.

favored in the direction of the polysilylene. Due to imperfect alignment of the polysilylene backbones in the oriented samples, this experimentally found anisotropy ratio of 9 is a lower limit.

From comparison of samples $A_\parallel$ and B in Figure 8 we see that $\Delta\sigma_{eop}/D$ increases by a factor of 2 if the drawn films are neatly aligned parallel to the microwave field instead of randomly placed in the microwave cell. From the end of pulse conductivity observed in earlier experiments[30] we have calculated a lower limit of the sum of the charge carrier mobilities of $\sum\mu_{min} = 1.5 \times 10^{-5}$ m$^2$ V$^{-1}$ s$^{-1}$ in the solid phase of 100% unoriented PDHS (sample D). Assuming that the effect of increasing the conductivity by a factor of 2 upon orienting the sample (i.e., going from B to $A_\parallel$) may be extrapolated to bulk PDHS, this leads to $\sum\mu_{min} = 3 \times 10^{-5}$ m$^2$ V$^{-1}$ s$^{-1}$ in the solid phase of PDHS in the direction of the silicon backbone.

From time of flight (TOF) measurements at room temperature on thin PDHS films, hole transport with a much smaller mobility of $3 \times 10^{-9}$ m$^2$ V$^{-1}$ s$^{-1}$ has been found.[49] However, it should be realized that the TOF technique measures the mobility of the charge carriers on a larger scale (micrometers). This drift mobility will be largely influenced by the effects of microscopic inhomogeneities due to the microcrystalline nature of the PDHS (domain boundaries, the presence of amorphous regions) as well as by effects of the electrode contacts. Also, chain to chain hopping of the charge carriers has to be included in the measured mobility.

The TRMC technique is a contactless method that probes the mobility of the charge carriers on a much smaller scale and will be mainly determined by charge transport along the polysilylene backbones. The mobility is probed by an oscillating field in the gigahertz range. Domain boundary effects and chain to chain hopping are therefore not necessarily included in the observed conductivity. As a result, the mobility determined by the TRMC technique will be mainly determined by charge transport along the polysilylene backbones, while the mobility as found from TOF measurements is mainly determined by the relatively slow transport of the charge carriers across domain boundaries and chain to chain hopping.

With the TRMC technique the sign of the charge carriers cannot be determined, and therefore a contribution of electron transport along the polysilylene backbones to the high conductivity observed in our measurements cannot be ruled out.

**Temperature Dependence of $\Delta\sigma_{eop}/D$.** In Figure 8, the temperature dependence of $\Delta\sigma_{eop}/D$ of samples A–D is shown. For $A_\perp$ no temperature-dependent data are given since the radiation-induced conductivity in the mesophase was too small to be measured accurately. All $\Delta\sigma_{eop}/D$ values are normalized to 100% PDHS. When the

conductivity at the end of the pulse ($\Delta\sigma_{eop}$) of $A_\parallel$ is determined, the fast-decaying part of the transients (that does not arise from the PDHS regions) is excluded by extrapolating the longer-lived PDHS signal to an end of pulse value as is indicated in Figure 7.

All samples show a sharp decrease of $\Delta\sigma_{eop}/D$ at the I → II transition at ±40 °C followed by a gradual increase above the transition temperature ($T_{I\rightarrow II}$). On cooling, the transition is found to be reversible with a hysteresis of ca. 15 °C. These phase transitions are also found from DSC measurements.

In the mesophase of samples B–D no differences in the crystallinities of the samples exist and the charge carrier mobilities are expected to be the same. The observed magnitude of $\Delta\sigma_{eop}/D$ in the mesophase is ca. $2.5 \times 10^{-8}$ $Sm^2/J$ for B–D when normalized with respect to PDHS content. This shows that this normalization is valid.

Sample B shows a somewhat higher value for $\Delta\sigma_{eop}/D$ compared with samples C and D. This can probably be attributed to the small amount of all-trans PDHS still present in the mesophase as was demonstrated by the small UV absorption band at 370 nm that was still present at 80 °C.

$\Delta\sigma_{eop}/D$ of sample $A_\parallel$ in the mesophase is $5 \times 10^{-8}$ $Sm^2/J$. A higher value of $\Delta\sigma_{eop}/D$ for sample $A_\parallel$ compared with the unoriented samples was expected on the basis of the alignment effects discussed above.

The considerably lower conductivity values found in the solid phases for samples A–C compared to that of sample D suggests that the polysilylene backbones cannot attain the perfect all-trans conformation in the solid phase. The conformational adjustment required appears to be hindered by the surrounding polyethylene, as was also found from DSC measurements and discussed above (Table I). We find that $\Delta\sigma_{eop}/D$ at room temperature correlates with the crystallinity calculated for the respective samples and therefore conclude that $\Delta\sigma_{eop}/D$ in phase I correlates with the amount of crystalline PDHS present. No direct proportionality should be expected since the crystallinity as found from DSC is mainly determined by the side-chain crystallization, while $\Delta\sigma_{eop}/D$ is determined by the main-chain conformation and may be very sensitive to small local conformational perturbations.

The solid to mesophase transition in the drawn samples $A_\parallel$ and B is not fully reversible, indicating some rearrangement of PDHS during the first heating/cooling cycle. However, annealing the oriented sample in the mesophase does not lead to a large loss of orientation of the polymer because after annealing the experimentally found anisotropy ratio of the sample is still close to a factor of 10.

**Conclusions.** Poly(di-*n*-hexylsilylene) was highly co-oriented in a matrix of UHMW-PE by gel blending and subsequent ultradrawing of the blend. TRMC experiments with oriented PE/PDHS films revealed an anisotropy ratio of at least an order of magnitude for charge transport in the direction of the oriented backbone and perpendicular to it. It is concluded that charge transport takes place preferentially along the highly oriented polymer backbones. A minimum value of the mobility of the charge carriers of $3 \times 10^{-5}$ $m^2$ $V^{-1}$ $s^{-1}$ is found in the solid phase of PDHS, which is 4 orders of magnitude higher than the hole drift mobility was found from TOF measurements.

The radiation-induced conductivity in the solid phase was found to correlate with the amount of PDHS present with all-trans backbone conformation.

These results may have interesting consequences for various applications of polysilanes based on their electroactive properties. Oriented molecular architectures can be expected to show considerably improved properties when compared with the properties as found from DC experiments on polycrystalline material without preferential orientation.

**Acknowledgment.** We are grateful to Dr. J. M. Warman, IRI, and Theo Jongeling, DSM, for valuable discussions. Furthermore, we thank Prof. Dr. H. Wendorff, Darmstadt, for making the dichroic UV experiments possible and Janka Czech for preparing the PE/PDHS blends and carrying out the DSC experiments. The present investigation was supported by the Dutch Ministry of Economic Affairs Innovation—Oriented Research Programme on Polymer Composites and Special Polymers (IOP-PCBP). H.F. acknowledges financial support by DSM-Research, Gelen, The Netherlands.

## References and Notes

(1) Wegner, G. *Polymer* **1992**, *33*, 3995.
(2) Wittmann, J. C.; Smith, P. *Nature* **1991**, *352*, 414.
(3) Embs, F. W.; Funhoff, D.; Laschewsky, A.; Licht, U.; Ohst, H.; Prass, W.; Ringsdorf, H.; Wegner, G.; Wehrmann, R. *Adv. Mater.* **1991**, *3* (1), Special Issue: Organic Thin Films.
(4) Embs, F. W.; Wegner, G.; Neher, D.; Albouy, P.; Miller, R. D.; Willson, C. G.; Schrepp, W. *Macromolecules* **1991**, *24*, 5068.
(5) Garnier, F.; Horowitz, G.; Peng, X.; Fichou, D. *Adv. Mater.* **1990**, *2*, 592.
(6) Park, Y. W.; Druy, M. A.; Chiang, C. K.; Heeger, A. J.; MacDiarmid, A. G.; Shirakawa, H.; Ikeda, S. *J. Polym. Sci., Polym. Lett.* **1979**, *17*, 195.
(7) Heeger, A. J.; Smith, P. In *Conjugated Polymers*; Brédas, J. L., Silbey, R., Eds.; Kluwer Academic Publishers: Dordrecht, 1991; p 201.
(8) de Haas, M. P.; Hummel, A.; Warman, J. M. *Synth. Met.* **1991**, *41*, 1255.
(9) de Haas, M. P.; Hummel, A. *IEEE Trans. Electr. Insul.* **1989**, *24* (2), 349.
(10) Miller, R. D.; Michl, J. *Chem. Rev.* **1989**, *89*, 1359.
(11) Miller, R. D.; MacDonald, S. A. *J. Imaging Sci.* **1987**, *31*, 43.
(12) Yokoyama, K.; Yokoyama, M. *Chem. Lett.* **1989**, 1005.
(13) Stolka, M.; Yuh, H.-J.; McGrane, K.; Pai, D. M. *J. Polym. Sci., Polym. Chem. Ed.* **1987**, *25*, 823.
(14) Abkowitz, M. A.; Stolka, M.; Weagley, R. J.; McGrane, K. M.; Knier, F. E. In *Silicon Based Polymer Science*: Zeigler, J. F., Fearon, F. W. G., Eds.; American Chemical Society: Washington, DC, 1990; pp 467–503.
(15) Abkowitz, M. A.; Rice, M. J.; Stolka, M. *Philos. Mag. B* **1990**, *61*, 25.
(16) Kido, J.; Nagai, K.; Okamoto, Y.; Skotheim, T. *Chem. Lett.* **1991**, 1267.
(17) Kakui, M.; Yokoyama, K.; Yokoyama, M. *Chem. Lett.* **1991**, 867.
(18) Kajzar, F.; Messier, J.; Rosilio, C. *J. Appl. Phys.* **1986**, *60*, 3040.
(19) Baumert, J. C.; Bjorklund, G. C.; Jundt, D. H.; Jurich, M. C.; Looser, H.; Miller, R. D.; Rabolt, J.; Sooriyakumaran, R.; Swalen, J. D.; Twieg, R. J. *Appl. Phys. Lett.* **1989**, *53*, 1147.
(20) Kaatz, P. G.; Patterson, G. D.; Kim, H. K.; Frey, H.; Matyjaszeki, *K. Mater. Res. Soc. Symp. Proc.* **1991**, *214*, 17.
(21) Herman, A.; Dreczewski, B.; Wojnowski, W. *Chem. Phys.* **1985**, *98*, 475.
(22) Trefonas, P., III; West, R.; Miller, R. D.; Hofer, D. *J. Polym. Sci., Polym. Lett. Ed.* **1983**, *21*, 823.
(23) Weber, P.; Guillon, D.; Skoulios, A.; Miller, R. D. *J. Phys. (Paris)* **1989**, *50*, 793.
(24) Varma-Nair, M.; Cheng, J.; Jin, Y.; Wunderlich, B. *Macromolecules* **1991**, *24*, 5442.
(25) Kögler, G.; Loufakis, K.; Möller, M. *Polymer* **1990**, *31*, 1538.
(26) Allcock, H. R. *Angew. Chem.* **1977**, *89*, 153.
(27) Tervoort, Y., Dissertation Eindhoven, The Netherlands, 1991.
(28) Möller, M.; Frey, H.; Sheiko, S. *Colloid Polym. Sci.* **1993**, *271*, 554.
(29) Smith, P.; Lemstra, P. J. *Colloid Polym. Sci.* **1980**, *257*, 891.
(30) Frey, H.; Möller, M.; de Haas, M. P.; Zenden, N. J. P.; Schouten, P. G. van der Laan, G. P.; Warman, J. M. *Macromolecules* **1993**, *26*, 89.
(31) van der Laan, G. P.; de Haas, M. P.; Warman, J. M.; Frey, H.; Möller, M. *Mol. Cryst. Liq. Cryst.* **1993**, *236*, 165.

(32) Miller, R. D.; Hofer, D.; Rabolt, J.; Fickes, G. N. *J. Am. Chem. Soc.* **1985**, *107*, 2172.
(33) Warman, J. M.; de Haas, M. P. In *Pulse Radiolysis*; Tabata, Y., Ed.; CRC Press: Boca Raton, FL, 1990; pp 101–132.
(34) Abkowitz, M. A.; Knier, F. E.; Yuh, H. J.; Weagley, R. J.; Stolka, M. *Solid State Commun.* **1987**, *62*, 547.
(35) Frey, H.; Matyjaszewski, K.; Möller, M.; Oelfin, D. *Colloid Polym. Sci.* **1991**, *269*, 442.
(36) Miller, R. D.; Thompson, D.; Sooriyakumaran, R.; Fickes, G. N. *J. Polym. Sci., Polym. Chem.* **1991**, *29*, 813.
(37) Smith, P.; Lemstra, P. J. *Makromol. Chem.* **1979**, *180*, 2983.
(38) Schouten, P. G.; Warman, J. M.; de Haas, M. P. *J. Phys. Chem.* **1993**, *97*, 9863.
(39) Infelta, P. P.; de Haas, M. P.; Warman, J. M. *Radiat. Phys. Chem.* **1977**, *10*, 353.
(40) Warman, J. M.; de Haas, M. P.; Wentinck, H. M. *Radiat. Phys. Chem.* **1989**, *34*, 581.
(41) Trefonas, P., III; Miller, R. D.; West, R. J. *J. Am. Chem. Soc.* **1985**, *107*, 2737.
(42) Karatsu, T.; Miller, R. D.; Sooriyakumaran, R.; Michl, J. *J. Am. Chem. Soc.* **1989**, *111*, 1140.
(43) Miller, R. D. *ACS Adv. Chem. Ser.* **1990**, 224, 413.
(44) Lovinger, A. J.; Padden, F. J.; Davis, D. D. *Polymer* **1991**, *32*, 3086.
(45) Sheiko, S. S.; Magonov, S. N.; Möller, M. *Polym. Prepr.* **1992**, *33* (1), 788.
(46) Harrah, L. A.; Zeigler, J. M. *Macromolecules* **1987**, *20*, 601.
(47) Warman, J. M. In *The Study of Fast Processes and Transient Species by Electron Pulse Radiolysis*; Baxendale, J. H., Busi, F., Eds.; Reidel: Dordrecht, Holland, 1982; pp 433–533.
(48) Unpublished results, IRI Delft.
(49) Abkowitz, M. A.; McGrane, K. M.; Knier, F. E.; Stolka, M. *Mol. Cryst. Liq. Cryst.* **1990**, *183*, 157.